Stage: I. Fabrication and characterization of mirrors

I.1. Preparation and characterization of metallic and dielectric mirrors for fs lasers

For the research topics of this project, we prepared both metallic (Ag) and dielectric (HfO_2 and ZrO_2) mirrors. Since PLD technique when applied to metallic targets results in the growth of thin films that have a high density of micrometer sized droplets, which will scatter the incident light and therefore interfere with the optical measurements of the Laser Induced Damage Threshold (LIDT) value, we decided to use radio-frequency magnetron assisted sputtering.

Ag thin films were obtained from a metallic Ag target and deposited onto glass and silicon substrates using the rfMS deposition technique. After deposition, the films structure was investigated using grazing incidence X-ray diffraction (GIXRD) and X-ray reflectivity (XRR). The surface morphology of the deposited films was investigated using scanning electron microscopy (SEM). Chemical composition of the films was investigated using X-Ray photoelectron spectroscopy (XPS). Dielectric films were been grown using PLD technique in two installations: one using a KrF laser (248 nm wavelength) and one using an ArF laser (193 nm). The oxygen pressure during deposition was around 1×10^{-2} mbar, a value that corresponds to the highest LIDT value previously measured.

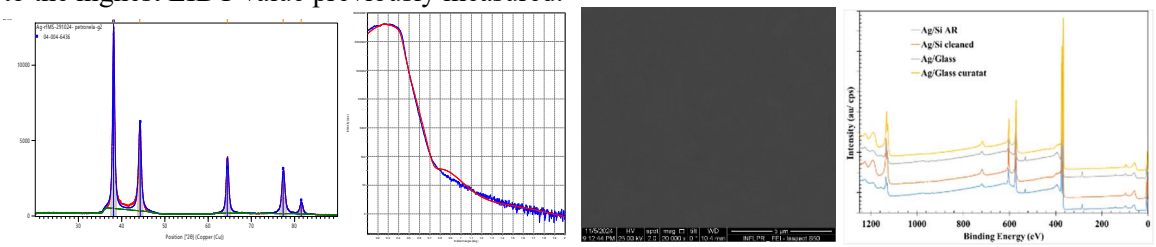

Fig. 1. GIXRD patterns of an Ag film (left) and the recorded XRR curve and its simulation (right); Fig. 2. SEM image of the Ag film. Fig. 3. XPS survey spectra recorded from Ag films deposited on Si and glass.

In Fig. 1 the GIXRD patterns and XRR curve (blue trace) and its simulation with the Panalytical software (blue trace) acquired from a typical Ag film are displayed. The vertical lines correspond to the reference diffraction pattern of Ag (04-004-6443, space group Fm-3m, 225) with a lattice parameter of a=4.0872 Å. According to our estimation the deposit film has an a=4.0882 Å and a grain size of 187 Å. The film's density was estimated from the XRR measurements to be 10.1 g/cm^3 with a surface roughness of 2.6 nm. The top view SEM images of silver films deposited on both glass and Si appeared smooth, homogeneous, and featureless at low magnification, as one can see in Fig. 2. The EDX and XPS analysis showed pure Ag films and small traces of oxygen, confirming the purity of the deposited Ag films (Fig. 3).

I.2 Vacuum compatible MCC & LP setup

In preparation for the electrical measurements of the LIDT, a preliminary design of the system was considered and corresponding acquisitions were performed. A 4-channel oscilloscope was acquired to measure the MCC and LP signals from the irradiated samples. The oscilloscope has external trigger input to make synchronous measurements with the laser pulses delivery.

I.3 Contamination processes: calibration and preparation

The contamination of the mirrors used in vacuum at different laser facilities is one of the factors that lead to damage to the mirrors. To mitigate this risk, we proposed a non-invasive method based on broadband source interferometry to investigate the contamination quantitatively. By monitoring the phase, group delay, and group delay dispersion of the mirrors, we were able to qualify the contamination as a function of coating design, deposition method, and contamination time in the vacuum chamber. The results were presented at the SPIE Laser Damage conference (most important event in LIDT in the world) and a conference proceeding was submitted.

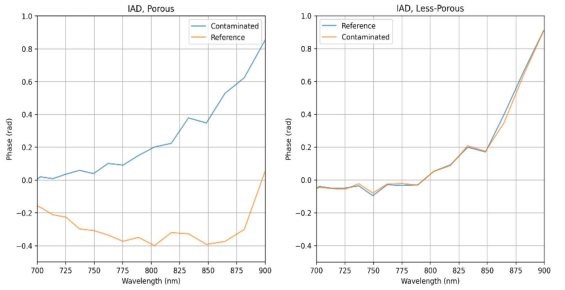

Figure 4: The influence of the contamination for different coating type Left)- porous, Right) less porous.

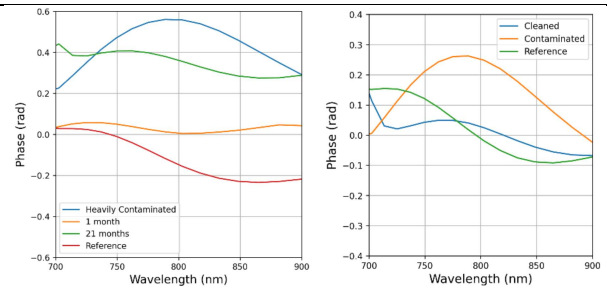

Left) Contamination in vacuum chamber, in time where Orange (1 month), Green (21 months); Blue (heavily contaminated) and Right) The recovery of the initial state after cleaning.

Complementary, we report the current observations of the carbonization problem in ELI-NP laser beamlines. All the beamlines of 0.1 to 10 PW had the carbonization of the beam transport mirrors at fs pulse in vacuum. We tested 3 different cleaning methods to remove this carbonization, namely the dip cleaning in the water-alcohol mixture, oxygen plasma cleaner, and pump down with silica gel. The dip cleaning was applied to 1 PW mirror to remove the contamination before the carbonization was observed. For the first time for large mirrors. The oxygen plasma can remove surface carbon, but it is not enough to remove the carbon inside the coating. Silica gel provides some slow pumping of the vacuum and some increase of low-mass gasses due to the increased surfaces. The method to identify the pass-way of the contamination into the vacuum chamber was proposed. The results were presented at the SPIE Laser Damage conference and a conference proceeding was submitted.

LIDT ns test station was used for preliminary tests to optimize station functioning. Metallic oxides coatings were used to test 1-on-1 method for different wavelengths. This method was choosen due to the fact that Damage detector (a critical element for S-on-1 tests) had an erratic mode of operation.

Below are some results for laser wavelength @ 532 nm. Laser station optics (which usually works on the 1064nm wavelength) were replaced/calibrated/aligned to the new wavelength. In the images below are presented the typical temporal and spatial pulse profiles for 532nm wavelength for the preliminary tests.

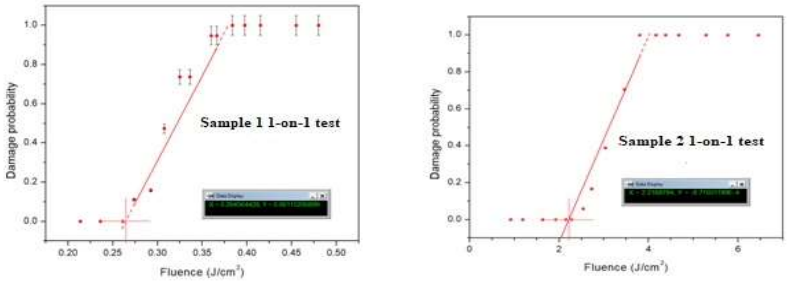

Figure 5. Linear fit results for damage threshold: $H_0(1) = 0.26^* J/cm^2$; $H_0(1) = 2.2^* J/cm^2$

Samples were cleaned by blowing with aerosol spray on both surfaces. Surface areas presented material dots and holes spots after blowing so perhaps method drag&drop can be used for a much better cleaning. The microscope DinoLite, focused on the sample, was used for damage detection. The damage points were then verified using Carl Zeiss AxioLab microscope. Values obtained were plotted in the figs. 5.

Contaminated samples were prepared using metallic mirrors (Ag on glass or Si wafers) as described in section I.1. Three carbon deposition methods simulated contamination: plasma-enhanced CVD (hydrocarbon decomposition in plasma), pulsed laser ablation (PLD) of a carbon target, and laser CVD (carbon particle formation via laser-induced hydrocarbon decomposition). Surface morphology (SEM, AFM), chemical composition, and depth distribution (XPS), as well as optical properties (ellipsometry), were analysed.

Amorphous hydrogenated carbon (a-CH) layers were deposited using plasma-enhanced chemical vapour deposition (PECVD) with argon (Ar) and methane (CH_4) at flow rates of 50 and 25 SCCM. The

resulting 10 nm film thickness indicated a growth rate of 1 nm/min, confirmed by Atomic Force Microscopy (AFM).

Compact and dense carbon layers were produced via PLD, where a laser beam interacts with a bulk graphite target, creating a plasma plume that deposits material onto the substrate. The process was conducted in a vacuum (1×10^{-5} mbar) using a YAG:Nd laser operating at 266 nm, 10 Hz, and a fluence of 3 J/cm². X-ray diffraction confirmed all layers were amorphous (data not shown).

To simulate "soot" type contaminants on the laser reflection mirrors, a CO2 continuous wave laser (λ=10.6 mm, power 350 W) was directed across a flow of gas consisting of an Ar carrier (flow rate of 2000 sccm) charged with a mixture of C_2H_2/C_2H_4 (with equal mass flow values of 50 sccm). The experiments proceeded inside a closed chamber kept at 800 mbar pressure. The carbon material (soot) resulting from hydrocarbon gas decomposition and gas phase reactions is transported by the gas flow and contaminates the mirror surfaces placed downstream, at about 50 cm distance from the reaction zone.

SEM images shown in Figure 6 demonstrate distinct morphologies of the initial and carbon-contaminated surfaces created by the PECVD, PLD, and laser-CVD methods, depending on the technique used for carbon contamination. AFM images of the initial, PECVD, and PLD carbon-contaminated mirrors exhibit smooth surfaces with distinct topographical features based on the contamination method. All investigated surfaces show a smoothness with roughness below 3 nm, with minimal variation based on the contamination method.

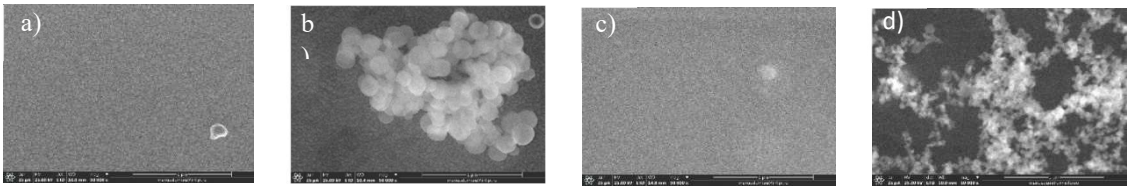

Figure 6. SEM images of initial (a) and carbon-contaminated mirrors by PECVD (b), PLD (c) and laser-CVD (d)

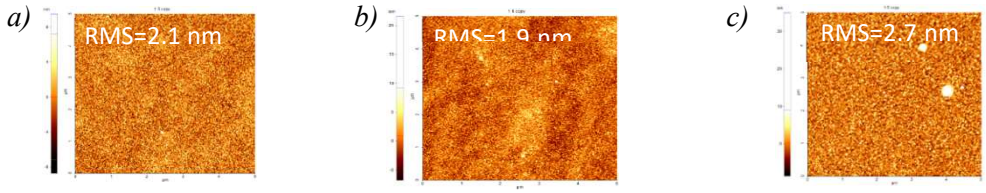

Figure 7. AFM images of initial (a) and PECVD (b) and PLD (c) carbon-contaminated substrates

Figure 8 presents an analysis of the depth profile of carbon-contaminated mirrors produced by PECVD, PLD, and laser-CVD methods.

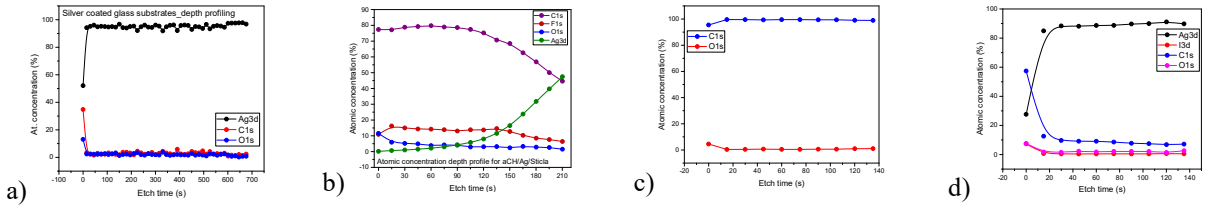

Figure 8. XPS depth profile of uncontaminated (a); and contaminated mirrors by PECVD (b); PLD (c); and laser-CVD (d) techniques.

In conclusion, mirrors were covered with carbon contaminants by a number a processes mimicking situations close to real contamination in laser experiments. The contaminant layers were characterized in respect to the morphology and chemical distribution at surface and in-depth. Samples were made available to be used in the next stages of the project where plasma will be used for cleaning surfaces.